ELSEVIER

Journal of Nuclear Materials 280 (2000) 162–168

journal of nuclear materials

www.elsevier.nl/locate/jnucmat

Irradiation-induced embrittlement of a 2.25Cr1Mo steel

S.-H. Song [a,*], R.G. Faulkner [b], P.E.J. Flewitt [c], R.F. Smith [c], P. Marmy [d], M. Victoria [d]

[a] *Department of Materials Engineering, Brunel University, Uxbridge, Middlesex UB8 3PH, UK*
[b] *Institute of Polymer Technology and Materials Engineering, Loughborough University, Loughborough, Leicestershire LE11 3TU, UK*
[c] *Berkeley Centre, BNFL Magnox Generation, Berkeley, Gloucestershire GL13 9PB, UK*
[d] *EPFL-CRPP, Fusion Technology, CH-5232 Villigen PSI, Switzerland*

Received 15 November 1999; accepted 17 March 2000

Abstract

Irradiation-induced embrittlement of a 2.25Cr1Mo is investigated by means of small punch testing and scanning electron microscopy (SEM). The ductile–brittle transition temperature (DBTT) determined by the small punch test is much lower than that determined by the standard Charpy test. There are some irradiation-induced embrittlement effects after the steel is irradiated at about 270°C for 46 days with a neutron dose rate of 1.05×10^{-8} dpa s^{-1} and at about 400°C for 86 days with a neutron dose rate of 1.75×10^{-8} dpa s^{-1}. In addition, there is some temper embrittlement after the steel is aged at about 400°C for 86 days.

1. Introduction

Irradiation-induced embrittlement of low-alloy steels employed in the nuclear power industry is a serious problem. This embrittlement manifests itself by an increase in ductile–brittle transition temperature (DBTT) and a reduction in upper-shelf energy (USE) [1]. The embrittlement may be classified into hardening embrittlement and non-hardening embrittlement [2]. Hardening embrittlement is caused by irradiation-induced defect clusters and copper or carbide precipitation. Non-hardening embrittlement is brought about by grain boundary segregation of impurities such as phosphorus.

Evaluation of irradiation-induced embrittlement is one of the major research activities in the field of radiation damage. Due to the limited space available in irradiation facilities and the difficulty in the handling of radioactive materials, it is popular [3] to utilise miniaturised specimens to evaluate the mechanical properties of a radioactive material. To examine the DBTT changes of a neutron-irradiated material, one usually uses the mini-Charpy and small punch tests. The mini-Charpy test is the same as the standard Charpy test except for the adoption of a miniaturised specimen. The small punch test is a relatively new technique and uses small samples, for example, disc-shaped specimens, to evaluate indirectly the tensile mechanical properties and fracture energy of a material. In the present work, embrittlement of a neutron-irradiated 2.25Cr1Mo steel was examined by the use of small punch and mini-Charpy testing techniques.

2. Experimental procedure

A nominal 2.25Cr1Mo steel was prepared by induction melting of the base elements under an argon atmosphere. The resulting ingots were hot-rolled to 10 mm diameter rods and they were then austenitised at 1150°C for 2 h, furnace cooled to a temperature of 950°C, held there for 1 h and then oil quenched. They were then toughened at 650°C for 2 h followed by water quenching. The toughening treatment was aimed at giving the material a ductile state and preparing a homogeneous microstructure for subsequent age and irradiation. The

* Corresponding author. Tel.: +44-1895 274 000 ext. 2984; fax: +44-1895 812 636.
E-mail address: shenhuasong@hotmail.com (S.-H. Song).

0022-3115/00/$ - see front matter
PII: S0022-3115(00)00042-8

Table 1
Chemical composition of 2.25Cr1Mo steel (wt%)

C	Mn	S	P	Si	Cr	Ni	Mo	Sn	As	Sb
0.086	0.46	0.010	0.039	0.27	2.28	0.15	1.00	0.01	0.005	0.01

rod samples heat-treated above were cut into quasi-prepared disc specimens 3 mm in diameter and 0.5 mm in thickness and machined into mini-Charpy V-notch specimens 3 mm × 4 mm × 27 mm in size, respectively. The quasi-prepared disc specimens were subsequently ground on the SiC polishing paper in the sequence of 240, 400, 600, 800, and 1200 grit down to a nominal thickness of 0.25 mm for use in the small punch test. The chemical composition of the steel is shown in Table 1.

Material irradiation was performed in a thermal light-water research reactor, named SAPHIR, operated by the Swiss Federal Institute for Reactor Research in Villigen (Switzerland). This reactor operates at a thermal power of 10 MW. The thermal neutron flux is 8×10^{13} n cm^{-2} s^{-1} at the core surface and up to 1.2×10^{14} n cm^{-2} s^{-1} in the central irradiation positions. In this work, the specimens were irradiated for 46 days with a neutron dose rate of about 1.05×10^{-8} dpa s^{-1} at about 270°C (fast neutron energy > 1 MeV) and for 86 days with a neutron dose rate of about 1.75×10^{-8} dpa s^{-1} at about 400°C (fast neutron energy > 1 MeV), respectively. To enable radiation effects to be distinguished from any purely thermal effects generated during irradiation, thermal control specimens were produced and aged by simulating the irradiation process.

The small punch test technique and jig were described in great detail in Ref. [4]. In brief, the test jig consists of a disc specimen and a specimen holder. The specimen holder is comprised of upper and lower dies, and four clamping screws. With the use of this specimen holder, the specimen is prevented from cupping upward during punching and plastic deformation is therefore concentrated in the region below the punch (ball bearing 1 mm in diameter). Fig. 1 gives a schematic diagram showing the test jig.

The small punch test was performed on a universal testing machine, Hounsfield H10KM, equipped with an environmental chamber cooled with liquid nitrogen. Each test was carried out at a constant crosshead speed of 0.1 mm min^{-1}. Two identical miniaturised disc jigs were used for testing. In the test, 3–6 specimens were adopted for each condition. Temperature was controlled by a chromel/alumel thermocouple placed in the environmental chamber and a second thermocouple was attached to the jig to measure the actual temperature of the jig. During testing, the load–displacement data were recorded at every 4 μm displacement and stored in a microcomputer that allowed the data to be subsequently processed.

To compare the ductile–brittle transition behaviour from small punch testing with that from Charpy testing, mini-Charpy testing was conducted on a mini-Charpy testing system designed and manufactured in EPFL-CRPP Fusion Technology, Villigen-PSI, Switzerland. It has been shown from a MANET II ferritic stainless steel [5] that the DBTT determined from the mini-Charpy test is approximately 50°C lower than that determined from the standard Charpy test. Since there is only limited material available, the mini-Charpy test was conducted only for 270°C aged and irradiated specimens and only one specimen was tested for each condition.

Fracture surfaces for thermally aged specimens were examined by means of a Cambridge Stereoscan 360 scanning electron microscopy (SEM) and those for irradiated specimens by means of a JSM-840A SEM.

3. Results and discussion

Typical load–displacement curves for both 270°C and 400°C aged and irradiated specimens are represented in Fig. 2. Clearly, the maximum load increases with decreasing temperature while the displacement at

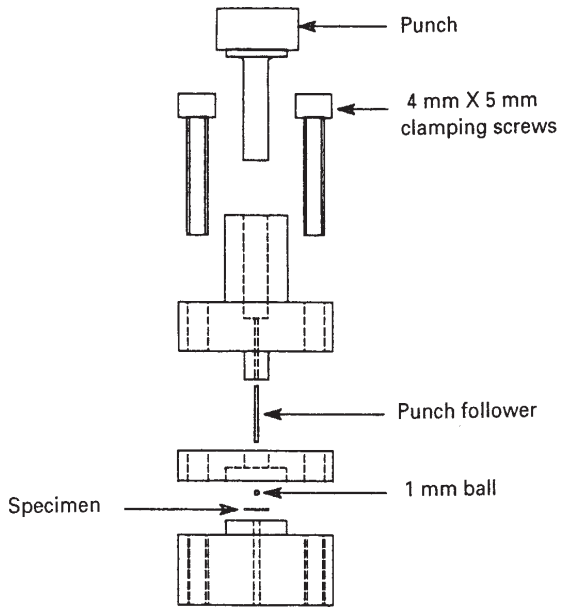

Fig. 1. Schematic diagram showing the test jig to test disc specimens 3 mm in diameter and 0.25 mm in thickness.

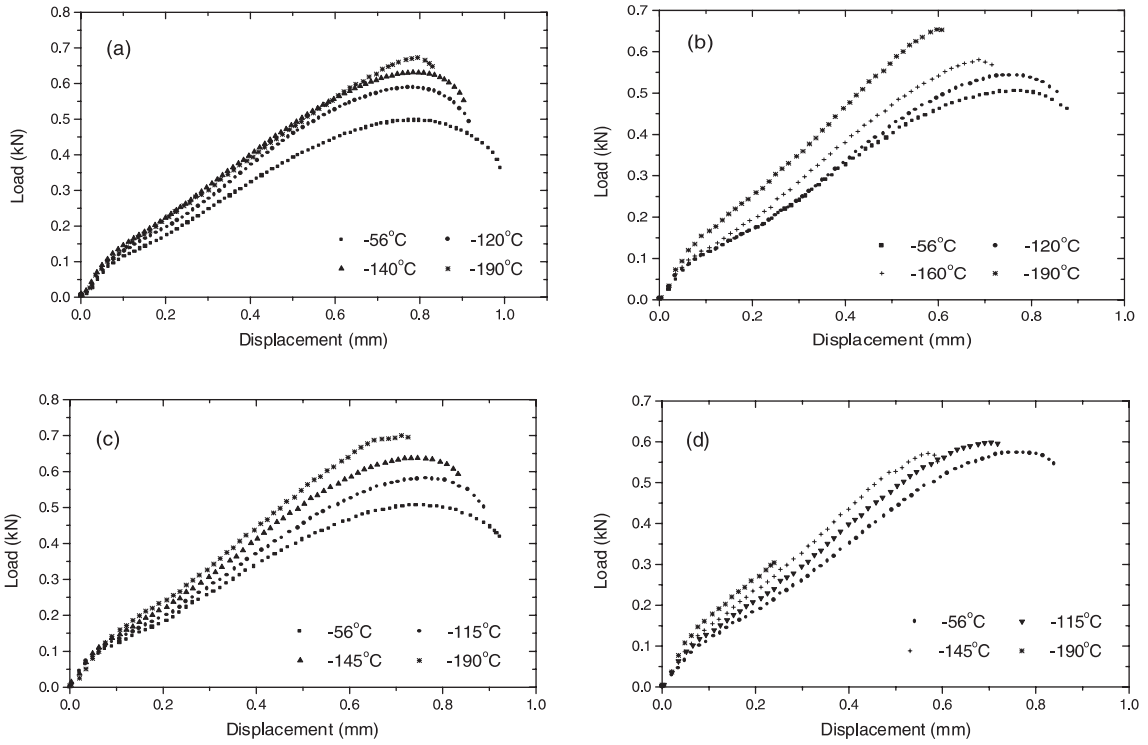

Fig. 2. Typical load–displacement curves for the specimens aged at: (a) 270°C and (c) 400°C, respectively, and irradiated at (b) 270°C and (d) 400°C, respectively, determined by the small punch test.

fracture decreases. In this work, a concept of the specific fracture energy (SFE) was used to normalise the fracture energy. The SFE is defined as the fracture energy per unit specimen thickness in units of mJ mm^{-1} and the fracture energy is determined by the area under the load–displacement curve in units of mJ. This is because the specimen thicknesses are slightly different from each other and are in the range of 0.235–0.255 mm. The SFE is shown in Fig. 3 as a function of test temperature for all the specimen conditions considered. Apparently, although the data have some scatter, the SFE decreases clearly, at a given test temperature, on going from 270°C-aging to 400°C-aging to 270°C-irradiating and to 400°C-irradiating, except in the test temperature range of below about −100°C for 270°C and 400°C-irradiated specimens. The SFE peak on the SFE–temperature curve shifts to higher temperatures in the same material condition sequence as above. In the test temperature range of above about −100°C, the SFE is, on average, slightly higher for the 400°C-irradiated specimens than for the 270°C-irradiated ones, but they are within experimental error.

Owing to the fact that, in the steel, solute atoms except carbon are almost immobile below 300°C, it is difficult for the 270°C-aging to cause embrittlement of the steel under non-irradiation circumstances although

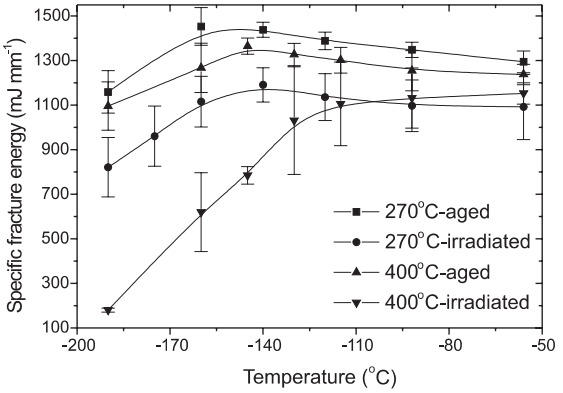

Fig. 3. SFE as a function of temperature for the specimens aged and irradiated at 270°C and 400°C, respectively, determined by the small punch test.

there might be a small amount of carbide precipitation. In this work, the 270°C-aged condition has been employed as the base for comparison although the 650°C-toughened condition should. It may be therefore concluded that neutron irradiation at 270°C and 400°C and aging at 400°C have given rise to embrittlement of the steel. If the SFE value for the 400°C-irradiated

specimens at −190°C is assumed to be the lowest value and the temperature corresponding to the arithmetic mean of the highest and lowest values to be the DBTT. The DBTT will be about −155°C for the 400°C-irradiated specimen. Since the SFE has not attained the lowest value until −190°C for the other specimens and it is difficult to conduct the test at temperatures below −190°C due to the limited cooling capability of the system, it is not feasible to determine the DBTT for these specimens from Fig. 3. However, it is definitely lower than −160°C for all the specimens and increases on going from 270°C-aging to 400°C-aging and to 270°C-irradiating. It may be seen also from Fig. 3 that, above the temperature corresponding to the SFE peak, the SFE increases with decreasing temperature. This is because, in this temperature regime, although the displacement at fracture decreases with decreasing temperature the maximum load increases dominantly, leading to an increase in SFE. As indicated in Refs. [4,6,7], such a shape of the SFE–temperature curve is typical in the small punch test.

To evaluate the yield strength (σ_y) of a material by means of the small punch test, Mao and Takahashi [8] have conducted both the small punch tests and the standard tensile tests for a series of ferritic steels and acquired the following empirical expression:

$$\sigma_y = \frac{0.36P_y}{t^2}, \tag{1}$$

where P_y is the yield load in N and t is the initial specimen thickness in mm. Both parameters can be directly obtained in the small punch test. In order to know clearly whether the embrittlement is partly contributed by hardening, this empirical expression has been employed to estimate the yield strength of the material for each test temperature. Fig. 4(a) represents the yield strength as a function of test temperature for the specimens aged and irradiated, respectively at 270°C. Clearly, there is no apparent difference between these two material conditions. This implies that the embrittlement caused by 270°C-irradiation is non-hardening embrittlement, i.e., it may be caused by grain boundary segregation of impurities such as phosphorus. The yield strength for the specimens aged and irradiated, respectively at 400°C is shown in Fig. 4(b) as a function of test temperature. The values for the 270°C-aged specimens are also plotted for comparison. Obviously, at a certain test temperature above about −140°C, the yield strength increases on going from 270°C-aging to 400°C-aging and to 400°C-irradiating. However, the yield strengths have no apparent difference at lower temperatures. As a consequence, both aging and irradiating at 400°C have brought about some hardening to the material. The hardening effect is somewhat larger for the 400°C-irradiated specimens. The aging-induced hardening may be caused by carbide precipitation during aging and the

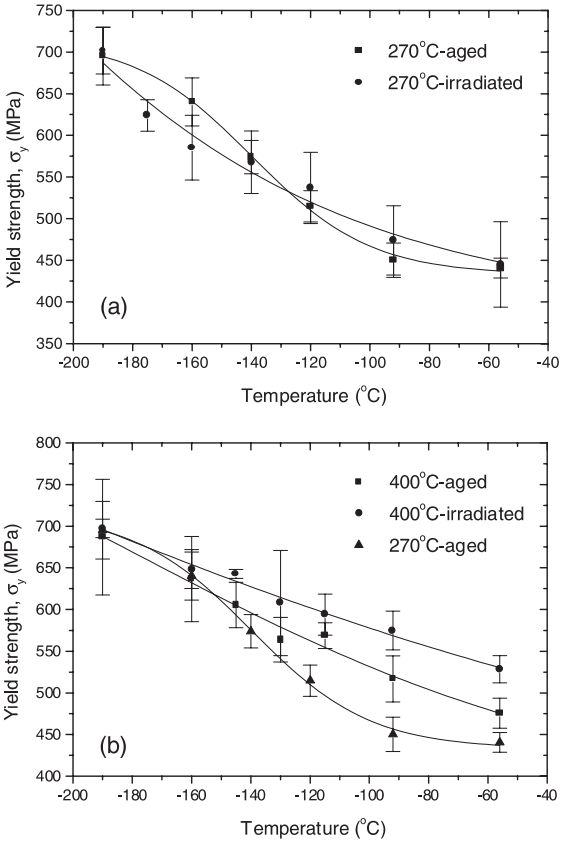

Fig. 4. Yield strength as a function of temperature: (a) for the specimens aged and irradiated, respectively at 270°C and (b) for the specimens aged and irradiated, respectively at 400°C with that for the 270°C-aged specimens plotted for comparison, determined by the small punch test.

irradiation-induced hardening by both carbide precipitation and defect cluster formation during irradiation. As it is well known [9,10], the yield stress of a crystal material increases with decreasing temperature or increasing shear modulus. Normally, the shear modulus of a material increases with decreasing temperature [4]. At lower temperatures, the hardening effect mentioned above may be therefore overwhelmed by the yield stress increase. It may be said that, in the present work, the hardening contribution to the embrittlement may be neglected at temperatures below about −140°C. This means that the difference in DBTT is mainly related to the non-hardening embrittlement mechanism, i.e., the impurity segregation-induced embrittlement, as the DBTTs determined by small punch testing are lower than −140°C for all the material conditions considered.

As mentioned above, since there is only limited material available, the mini-Charpy tests were performed only for the specimens aged and irradiated, respectively at 270°C. Fig. 5 shows the Charpy impact energy as a

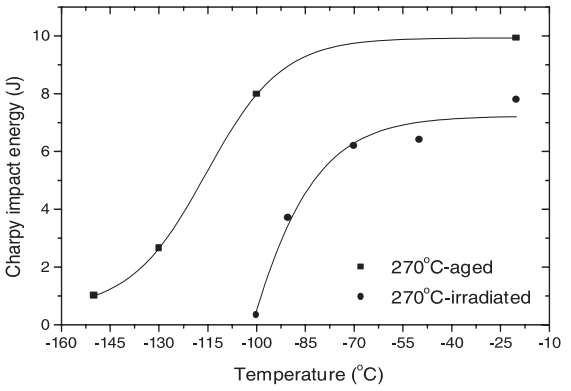

Fig. 5. Fracture energy as a function of temperature for the specimens aged and irradiated, respectively at 270°C, determined by the mini-Charpy test.

function of test temperature. Clearly, the ductile–brittle transition can be seen although the data points are too few. Due to irradiation, the DBTT is shifted to a higher temperature and the upper-shelf energy is decreased to a lower value. This is in reasonable agreement with the information acquired from the SFE–temperature curves (Fig. 3). If the temperature corresponding to the mean value of the highest and lowest Charpy impact energies is taken as the DBTT, the DBTT will be about −115°C for the 270°C-aged specimens and about −88°C for the 270°C-irradiated specimens. The irradiation-induced DBTT increase is about 27°C. Assuming the DBTT value gained from the mini-Charpy test to be about 50°C lower than that determined by the standard Charpy test [5], we can obtain that the standard DBTT is about −65°C for the 270°C-aged specimens and about −38°C for the 270°C-irradiated specimens. The DBTT of −65°C is just consistent with that acquired by Wada and Hagel [11] using the standard Charpy test with a similar material treated by a similar heat-treatment cycle. The work by Kameda and Mao using a series of ferritic steels with square specimens 0.5 or 0.25 mm in thickness [6] indicates the following empirical relationship between the DBTTs determined by the small punch test and by the standard Charpy test

$$(\mathrm{DBTT})_{\mathrm{SPT}} = 0.4(\mathrm{DBTT})_{\mathrm{SCT}}, \tag{2}$$

where $(\mathrm{DBTT})_{\mathrm{SPT}}$ is the DBTT in K, determined by the small punch test and $(\mathrm{DBTT})_{\mathrm{SCT}}$ is the DBTT in K, determined by the standard Charpy test. As a result, the $(\mathrm{DBTT})_{\mathrm{SPT}}$ might be about −190°C (83 K) for the 270°C-aged specimen and about −179°C (94 K) for the 270°C-irradiated specimen. It is worth mentioning that a theoretical analysis has demonstrated [12] that the $(\mathrm{DBTT})_{\mathrm{SPT}}$ decreases with decreasing applied strain rate. The small punch tests by Kameda and Mao were carried out with a crosshead speed in the range of 1.20–1.98 mm min^{-1} while ours is 0.1 mm min^{-1}. In our case, the factor in front of $(\mathrm{DBTT})_{\mathrm{SCT}}$ in Eq. (2) should be therefore smaller than 0.4. This implies that the $(\mathrm{DBTT})_{\mathrm{SPT}}$ should be lower than −190°C for the 270°C-aged specimens and −179°C for the 270°C-irradiated specimens. This is reasonably consistent with the information extracted from the SFE–temperature curves (Fig. 3). It should be noted that, owing to the fact [6] that there is a consistence between the small punch tests with square specimens and with disc ones in evaluation of yield strength (σ_y), ultimate tensile strength (σ_u), and fracture toughness (J_{1c}), we have assumed in the above discussion that there is also such a consistence in evaluation of DBTT. Also, it is worthy of note that the 50° difference between the DBTTs from the mini-Charpy and standard-Charpy tests is acquired from a MANET II ferritic stainless steel and the difference between them might be somewhat different for low-alloy steels.

In order to understand the micromechanisms of fracture, fracture surfaces of both small-punch and mini-Charpy tested specimens were examined by means of SEM. In general, the steel presents almost complete

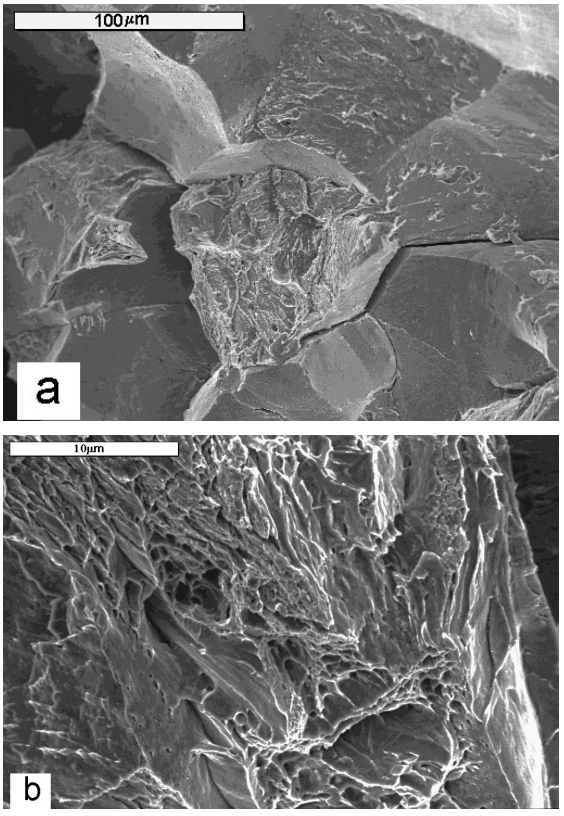

Fig. 6. Typical SEM fractographs for: (a) the 400°C-irradiated specimens small-punch-tested at −145°C; (b) the 270°C-aged specimens small-punch-tested at −190°C.

ductile fracture above the temperature corresponding to the SFE peak and mixed ductile and brittle fracture below this temperature with the amount of brittle fracture increasing with decreasing temperature until almost complete intergranular fracture. At a given test temperature, the fracture appears to be more brittle for the 400°C-irradiated specimens than for the other specimens. For instance, the specimens irradiated at 400°C exhibit almost complete intergranular fracture at −145°C, but the specimens aged at 270°C present mixed cleavage and ductile fracture even at −190°C (Fig. 6).

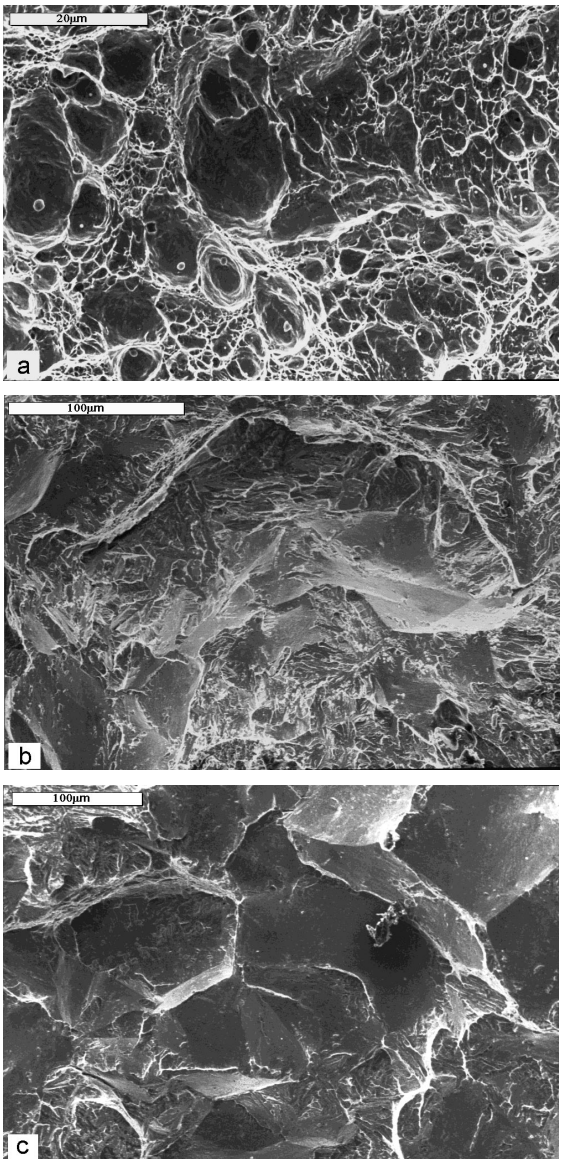

Fig. 7. Typical SEM fractographs for the 270°C-aged specimens mini-Charpy-tested at different temperatures: (a) −100°C; (b) −130°C; (c) −150°C.

This trend has also been confirmed by Bulloch [7]. Intergranular fracture is correlated with impurity segregation to grain boundaries. Therefore, there should be some irradiation-induced impurity segregation to grain boundaries in the steel. The information from SEM fractography is in reasonable conformity with that from the SFE–temperature curves (Fig. 3).

Typical SEM fractographs for the mini-Charpy specimens aged at 270°C and tested at −100°C, −130°C, and −150°C are shown in Fig. 7. Clearly, the steel exhibits almost complete ductile fracture at −100°C, almost complete cleavage fracture at −130°C, and intergranular fracture with a small amount of cleavage fracture at −150°C. As a consequence, the DBTT is definitely between −100°C and −130°C. This is in agreement with the information derived from the Charpy impact energy–temperature curve (Fig. 5). Predictions of combined equilibrium and non-equilibrium solute segregation to prior-austenite grain boundaries [13] have demonstrated that there has already been apparent phosphorus segregation in the steel during the 650°C-toughening treatment. This might be the reason why the material tempered at 270°C exhibits a large amount of intergranular fracture at −150°C, which is in the lower-shelf region on the Charpy impact energy–temperature curve. However, the SEM fractographs for the small punch specimens tempered at 270°C exhibit no intergranular fracture, even if tested at −190°C. There appears to be some contradiction in fractography between the small punch and mini-Charpy tested specimens. Nevertheless, if considering the lower-shelf region in the SFE–temperature curve, there would not be this contradiction. This is because the lower-shelf region in the SFE–temperature curve for the specimens tempered at 270°C is in a temperature range much below −190°C (Fig. 3) so that the material does not contain some intergranular fracture until −190°C in the small punch tests. If the tests were conducted at a lower temperature, leading to a lower SFE, there might be some intergranular fracture.

4. Summary

Embrittlement of low-alloy steels used in the nuclear industry is classified into hardening embrittlement and non-hardening embrittlement. Hardening embrittlement is caused by irradiation-induced defect clusters and copper or carbide precipitation. Non-hardening embrittlement is caused by grain boundary segregation of impurities such as phosphorus. Both thermal and irradiation effects at irradiation temperature are involved in both types of embrittlement. Embrittlement of a 2.25Cr1Mo steel aged and neutron-irradiated at about 270°C and 400°C, respectively, is evaluated by means of small punch testing. The DBTT determined by the small

punch test is much lower than that determined by the standard Charpy test. There is some irradiation-induced embrittlement after the steel is irradiated at about 270°C for 46 days with a neutron dose rate of 1.05×10^{-8} dpa s^{-1} or at about 400°C for 86 days with a neutron dose rate of 1.75×10^{-8} dpa s^{-1}. Also, there is some temper embrittlement after the steel is aged at about 400°C for 86 days. SEM fractography demonstrates a reasonable fit with the information derived from the small punch test results.

Acknowledgements

This work was supported by BNFL Magnox Generation and is published with the permission of the Director of Technology and Central Engineering Division of BNFL Magnox Generation. Also, we are indebted to Mr Frank Page of Loughborough University and Mr Nick Mayley-Jones of BNFL Magnox Generation for helping in SEM.

References

[1] L.K. Mansur, in: G.R. Freeman (Ed.), Kinetics of Non-Homogeneous Processes, Wiley, New York, 1987, p. 377.
[2] W.J. Phythian, C.A. English, J. Nucl. Mater. 205 (1993) 162.
[3] P. Jung, A. Hishinuma, G.E. Lucas, H. Ullmaier, J. Nucl. Mater. 232 (1996) 186.
[4] V. Vorlicek, L.F. Exworthy, P.E.J. Flewitt, J. Mater. Sci. 30 (1995) 2936.
[5] P. Marmy, EPFL-CRPP Fusion Technology, Villigen-PSI, Switzerland, private communication.
[6] J. Kameda, X. Mao, J. Mater. Sci. 27 (1992) 983.
[7] J.H. Bulloch, Int. J. Pres. Ves. Piping 63 (1995) 177.
[8] X. Mao, H. Takahashi, J. Nucl. Mater. 150 (1987) 42.
[9] F.R.N. Nabarro (Ed.), Dislocations in Solids, vol. 4: Dislocations in Metallurgy, North-Holland, Amsterdam, 1979.
[10] R.W. Cahn, P. Haasen, E.J. Kramer (Eds.), Materials Science and Technology, vol. 4: Structure in Solids, VCH Publishers, New York, 1993.
[11] T. Wada, W.C. Hagel, Metall. Trans. A 7 (1976) 1419.
[12] J. Kameda, Acta. Metall. 34 (1986) 2391.
[13] S.H. Song, R.G. Faulkner, P.E.J. Flewitt, J. Mater. Sci., submitted.